# Optimization of Minimum Negative Current BCM Synchronous Buck Converter

Yu Tang, *Senior Member, IEEE*, Chong Zhang, Yingjun Guo,
Hexu Sun, *Senior Member, IEEE* and Lin Jiang, *Senior Member, IEEE*

***Abstract*—Non-isolated DC-DC converters are widely used in renewable energy applications, such as the hybrid energy storage system (HESS), charging and discharging system of batteries and supercapacitors and the photovoltaic power generation. With the advantages of achieving zero-voltage-switching (ZVS), high efficiency and power density, low cost, and fast dynamic response, the converters operating in boundary current mode (BCM) have caught researchers' eyes recently. Taking the synchronous buck converters as an example, this paper briefly introduces the working principle and advantages of BCM converter realize soft switching. Firstly, it is pointed out that the phenomenon of circulating energy exists in the BCM converter. Then, the relationship between circulating energy and negative current is analyzed, and an optimal control strategy of negative current minimization is proposed to reduce the circulating energy. In the condition of realizing ZVS, negative current minimization not only improves the efficiency of the converter, but also reduces the ripple of inductor current to a certain extent. Finally, the experimental platform of 100 W synchronous buck converter is built. Experimental results validate that the optimal control of minimum negative current has good effect on improving efficiency of converter and reducing the ripple of inductor current.**

***Index Terms*—Soft-switching, boundary current mode, circulating energy, minimum negative current optimization**

## I. Introduction

Non-isolated DC-DC converters are widely used in the field of the hybrid energy storage system (HESS), charging and discharging system of batteries and supercapacitors and the photovoltaic power generation because of their simple structure and high efficiency [1]-[3]. In order to improve the efficiency and power density of converters, the implementation of soft-switching technology in DC-DC converter has become one of the research hotspots.

At present, the soft-switching technology applied to DC-DC converter can be divided into two categories. The first is the soft-switching technology with auxiliary circuits [4]-[6]; The second is controlled soft-switching technology [7]-[9].

The soft-switching technology of adding auxiliary circuit is a way to realize soft switching by adding some additional auxiliary components, such as resonant inductors, resonant capacitors and auxiliary switch, etc. A new family of soft-switching resonant dc-dc converters is presented in [4], the proposed topologies include only one switch, two diodes and one high-frequency resonant LC tank. Unlike quasi-resonant converters and soft-transition (ZVT/ZCT) converters, the proposed converter has only small resonant inductor and improves the power density of the converter. In [5], a new family of zero-voltage-transition (ZVT) bidirectional converters is proposed. The auxiliary circuit is composed of a coupled inductor with the converter main inductor and two auxiliary switches. The proposed converter provides soft-switching condition for all semiconductor elements without any extra voltage and current stress on the main switches. A new lossless passive snubber for the bidirectional buck/boost converter is introduced in [6]. The proposed snubber comprises a low number of passive components which jointly contribute to achieve soft switching condition at both the buck and boost operations of the converter.

Controlled soft-switching technology is a method to realize soft switching by controlling the electrical quantities in the topology, such as inductive current, and using the parasitic parameters of the topology. In [7], a mode of operation is proposed for PFC to control the inductor current to be the triangular-shaped, which is called triangular current mode (TCM). Furthermore, a simplified model of the nonlinear MOSFETs' output capacitances during working is also proposed. A high-frequency high-efficiency GaN device-based interleaved critical current mode (CRM) bidirectional buck/boost converter with an inverse coupled inductor is proposed in [8]. It is analyzed in detail that the range of soft switching is expanded in the case of inverse coupled inductor.
In [9], a soft switching technique for dc/ac inverters is proposed. ZVS is achieved through controlling the inductor current bidirectional in the set upper and lower current envelope in every switching cycle. This technique requires no additional resonant components and can be employed for various low power applications on conventional full-bridge and half-bridge inverter topologies. A high-frequency driver IC for gallium nitride (GaN) synchronous buck converter is proposed in [10], which minimizes dead-time at any load condition by means of adaptive bang-bang dead-time control. In [11], an accurate, uniform, and simple variable on-time (VOT) expression is presented for CRM PFC, and only an inverse signal of the rectified input voltage is additionally introduced to achieve accurate VOT control, which optimizes the THD of input current.

Compared with the soft-switching technology with auxiliary circuit, the controlled soft switching technology has the

advantages of high-power density, low cost and fast dynamic response. Currently, BCM is mainly used in PFC and inverter [9], [12]-[14], and there is little research on BCM DC-DC converter. Therefore, taking synchronous buck converters as an example, this paper applies BCM to DC-DC converters. In Section II, the phenomenon of the circulating energy in BCM converter is indicated. Then, the relationship between negative current and circulating energy is discussed, and the optimization scheme of the circulating energy and the ripple of inductor current is proposed in Section III, which is entitled optimal control strategy of minimum negative current. The feasibility of BCM realizes soft switching and optimization effect of minimum negative current are verified by experimental results in Section IV. The conclusion is presented in the last section.

## II. The Phenomenon of Circulating Energy of BCM Converter

Fig. 1 illustrates a BCM synchronous buck converters, taking into account the parasitic capacitors $C_1$ and $C_2$ and the body diodes $D_1$ and $D_2$ of the switches $S_1$ and $S_2$ in the synchronous buck converters.

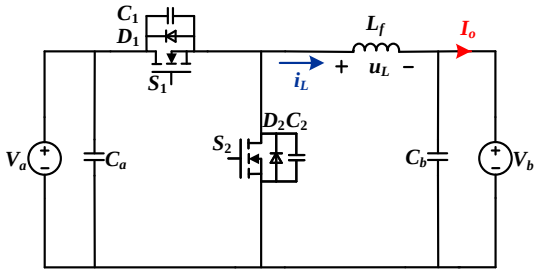


Fig. 1. The topology of BCM synchronous buck converters.

Fig. 2 shows the working waveforms of BCM synchronous buck converters.

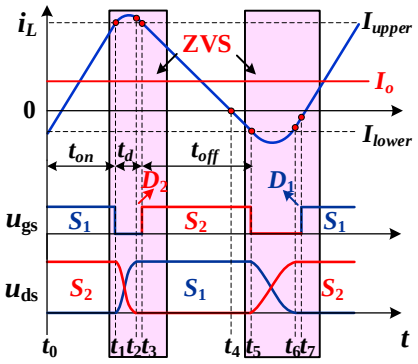


Fig. 2. The working waveforms of BCM synchronous buck converters (D<0.5).

The two switches $S_1$ and $S_2$ in the BCM synchronous buck converters are turned on alternately. During the deadtime, the parasitic capacitors and the body diodes of the MOSFETs and the output linear inductor are combined together to form a resonant circuit. The inductor current is intentionally realized bidirectional flow by current closed-loop control within a switching cycle to generate ZVS conditions during commutations.

The upper and lower limits of inductor current $I_{upper}$ and $I_{lower}$ can be calculated as follows:

$$\begin{cases} I_{upper} = 2I_o + I_R \\ I_{lower} = -I_R \end{cases} \tag{1}$$

where, $I_o$ is the output current, $I_R$ is the fixed reverse current for achieving ZVS.

The current lower limit $I_{lower}$ should be as large as possible to ensure the realization of soft switch. Therefore, $I_R$ must also be met:

$$I_R \geq \sqrt{\frac{2 \cdot C_{oss} V_a^2}{L_f}} \tag{2}$$

The fixed reverse current $I_R$ is positively associated with the equivalent capacitance $C_{oss}$ and inversely correlated with the filter inductor $L_f$. The larger output capacitance $C_{oss}$, the more obvious the buffering effect of turn-off, which is beneficial to reduce the loss of turn-off. The smaller the filter inductance, the higher the power density of the converter. Therefore, $I_R$ will be large, when $V_a$ = 200V, $C_{oss}$ = 462pF and $L_f$ = 40 μH, it is calculated that $I_R$ is equal to 1A.

Fig. 3 demonstrates the phenomenon of circulating energy in BCM converter.

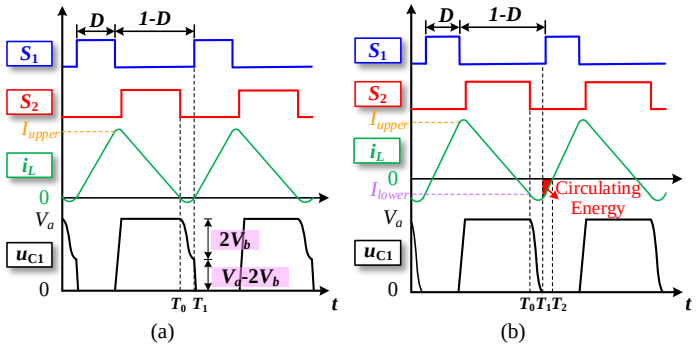


Fig. 3. The comparison between waveforms of CRM and that of BCM for synchronous buck converter ($D$<0.5). (a) CRM operation. (b) BCM operation.

Synchronous buck converter operating in CRM is presented in Fig. 3(a). When duty cycle $D$ < 0.5, the switch $S_1$ cannot realize ZVS, which is only turned on at the valley point. While, synchronous buck converter operating in BCM is shown in Fig. 3(b). When duty cycle $D$ < 0.5, the energy is stored in the filter inductor $L_f$ by allowing inductor current to flow negatively, which is used to neutralize capacitive reactive power of the parasitic capacitor to achieve ZVS in dead zone. Therefore, compared with CRM converter, BCM converter can realize ZVS within the full range of the output voltage.

However, synchronous buck converter operating in BCM exists the phenomenon of circulating energy due to inductor current flows negatively, as is illustrated in Fig. 3(b). After the time $T_1$, the switch $S_1$ (or the body diode $D_1$) is turned on, and the energy of main circuit flows from the output side to the input side until the time $T_2$, which generates reactive power loss in main circuit. In order to reduce reactive power loss, the relationship between the phenomenon of the circulating energy and control parameters of BCM is discussed, and the optimization scheme is proposed in this paper. Finally, the feasibility and effectiveness of the optimization scheme are verified by experimental results.

## III. Optimal Control Strategy of Minimum Negative Current

### A. The Analysis of Key Mode of the Deadtime

As shown in Fig.2, the zones [$t_1$-$t_3$] and [$t_5$-$t_7$] are the key modes for BCM converters to realize ZVS. In the two modes, all of the power switches are turned off, and the main circuit enters the dead zone.

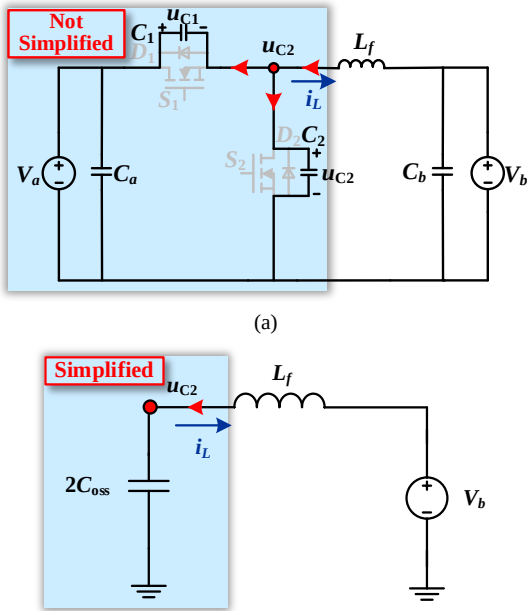


Fig. 4. The circuit diagram of realizing soft-switching. (a) The circuit of key mode. (b) The simplified circuit of key mode.

Take the zone [$t_5$-$t_7$] as an example since the analysis process of the two modes are similar, and the circuit diagram of the zone [$t_5$-$t_7$] is shown in Fig.4 (a). At this time, $i_L$ begins to discharge $C_1$ of $S_1$ and charge $C_2$ of $S_2$. Until $t_6$, $C_1$ completely discharges. Assuming that $C_1$ = $C_2$ = $C_{oss}$, $C_{oss}$ is the equivalent output capacitance of the power switches, and the simplified circuit is illustrated in Fig.4 (b). According to the simplified circuit, the mathematical derivation process of the drain-source voltage $u_{C2}$ of the switch $S_2$ as follows:

$$L_f \cdot 2C_{oss} \cdot \frac{d^2 u_{C2}}{dt^2} + u_{C2} = V_b \tag{3}$$

where, $L_f$ is the value of filter inductor, $V_b$ is the output voltage of BCM converters.

The initial condition (at the $t_5$) can be obtained from the initial working state of the circuit and the non-sudden change of capacitor voltage and inductor current:

$$\begin{aligned} u_{C2}(t)\big|_{t=t_5^+} &= u_{C2}(t_5^-) = 0 \\ i_L(t)\big|_{t=t_5^+} &= 2 \cdot C_{oss} \frac{du_{C2}}{dt}\bigg|_{t=t_5^+} = i_L(t_5^-) = I_{lower} \end{aligned} \tag{4}$$

The expression of the drain-source voltage $u_{C2}$ of the switch $S_2$ can be obtained by bringing the initial conditions into the equation (3):

$$u_{C2} = V_b - \sqrt{V_b^2 + \frac{I_{lower}^2 \cdot L_f}{2 \cdot C_{oss}}} \cdot \cos\left( \frac{t}{\sqrt{2 \cdot C_{oss} \cdot L_f}} + \lambda \right) \tag{5}$$

According to KVL, the drain-source voltage $u_{C1}$ of switch $S_1$ is:

$$\begin{aligned} u_{C1} &= V_a - u_{C2} \\ &= V_a - V_b + \sqrt{V_b^2 + \frac{I_{lower}^2 \cdot L_f}{2 \cdot C_{oss}}} \cdot \cos\left( \frac{t}{\sqrt{2 \cdot C_{oss} \cdot L_f}} + \lambda \right) \end{aligned} \tag{6}$$

where, $V_a$ is the input voltage of BCM converters.

Among $\lambda$ is:

$$\lambda = \arctan\left( \frac{I_{lower} \cdot \sqrt{\frac{L_f}{2 \cdot C_{oss}}}}{V_b} \right) \tag{7}$$

### B. The Relationship Between Circulating Energy and Negative Current $I_{lower}$

As shown in (a) zones [$t_6$-$t_7$] and (b) zones [$t_7$-$t_8$] of Fig. 5, the inductor current flows negatively. After the time $t_6$, the body diode $D_1$ or the switch $S_1$ is turned on. However, at the time $t_6$, inductor current $i_L$ remains negative and the energy of main circuit flows from the output side to the input side until the time $t_7$, which is the phenomenon of the circulating energy. As can be seen from Fig. 5(c), there must be a certain relationship between the negative current and the circulating energy, which is discussed as follow:

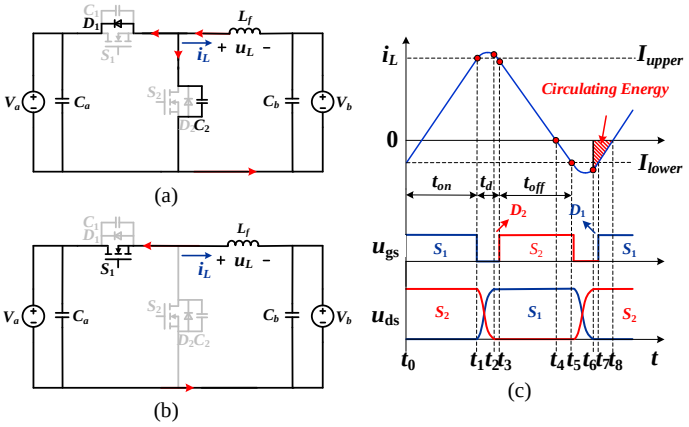


Fig. 5. The phenomenon of circulating energy. (a) The zones [$t_6$-$t_7$]. (b) The zones [$t_7$-$t_8$]. (c) The area of the circulating energy.

The expression of $i_L(t)$ in the zones [$t_5$-$t_6$] can be deduced from formula (5):

$$\begin{aligned} i_L(t) &= 2 \cdot C_{oss} \cdot \frac{du_{C2}}{dt} \\ &= \sqrt{\frac{2 \cdot C_{oss} \cdot V_b^2}{L_f} + I_{lower}^2} \cdot \sin\left( \frac{t}{\sqrt{2 \cdot C_{oss} \cdot L_f}} + \lambda \right) \end{aligned} \tag{8}$$

At the $t_6$, $u_{C1}$ drops to zero, and the inductor current $i_L(t_6)$ is:

$$i_L(t)\big|_{t=t_6} = -\sqrt{I_{lower}^2 - \frac{2 \cdot C_{oss} V_a (V_a - 2 \cdot V_b)}{L_f}} \tag{9}$$

After the time $t_6$, the value of inductor current $i_L(t)$ linearly changes from negative to positive, and the expression of inductor current $i_L(t)$ as follow:

$$i_L(t) = i_L(t_6) + \frac{V_a - V_b}{L_f} \cdot \Delta t \tag{10}$$

Until the time $t_8$, the energy of main circuit begins to flows from the input side to the output side, which means the

process of circulating energy is complete. Thus, the power of circulating energy is:

$$P_{\text{cir}} = \frac{1}{2}\cdot(V_a - V_b)\cdot\sqrt{I_{lower}^2 - \frac{2\cdot C_{oss} V_a (V_a - 2\cdot V_b)}{L_f}} \tag{11}$$

According to equation (11), it can be found that the smaller the lower limit of inductor current $I_{lower}$ is, the smaller the power of circulating energy is. However, according to equation (6), the prerequisite must also be met to ensuring the realization of soft switch:

$$V_a - V_b \le \sqrt{V_b^2 + \frac{I_{lower}^2 \cdot L_f}{2\cdot C_{oss}}} \tag{12}$$

According to equations (12), the greater the negative current $I_{lower}$ is, the easier soft-switching is realized.

### C. Optimal Control of Minimum Negative Current

Since the circulating energy increases the power loss of the converter and reduces the efficiency of the converter, especially for medium and small power converters, the reduction of circulating energy has become a key point to improve the efficiency of BCM converters.

An optimal control strategy of minimum negative current is proposed in this paper. The basic principle of the optimal control strategy is to minimize the circulating energy in the condition of realizing ZVS.

According to formula (12), when the following equation is satisfied, the negative current and circulating energy are minimized in the condition of realizing ZVS.

$$V_a - V_b = \sqrt{V_b^2 + \frac{I_{lower}^2 \cdot L_f}{2\cdot C_{oss}}} \tag{13}$$

At this time, the absolute value of negative current $I_{lower}$ reaches the minimum value $I_{min}$, that is:

$$I_{\min} = \sqrt{\frac{2\cdot C_{oss}\cdot V_a \cdot (V_a - 2\cdot V_b)}{L_f}} \tag{14}$$

Due to duty cycle $D = V_b / V_a$, the absolute value of the minimum negative current is:

$$I_{\min} = V_a \cdot \sqrt{\frac{2\cdot C_{oss}\cdot(1-2\cdot D)}{L_f}} \tag{15}$$

According to the obtained minimum negative current $I_{min}$, the dead time $t_d$ can be calculated as:

$$t_d = \left[\pi - \arctan\left(\frac{I_{\min}\cdot\sqrt{\frac{L_f}{2\cdot C_{oss}}}}{V_b}\right)\right]\cdot\sqrt{2\cdot C_{oss}\cdot L_f} \tag{16}$$

When the equivalent output capacitance of the power switches $C_{oss}$ = 462 pF and the filter inductor $L_f$ = 40 μF, Fig. 6 plots the relationship curve between the minimum negative current $I_{min}$ and duty cycle $D$. When duty cycle $D \ge 0.5$, BCM converters can realize ZVS without negative current, which is similar to CRM converters. When duty cycle $D < 0.5$, the minimum negative current $I_{min}$ increases with the decrease of the output voltage $V_b$.

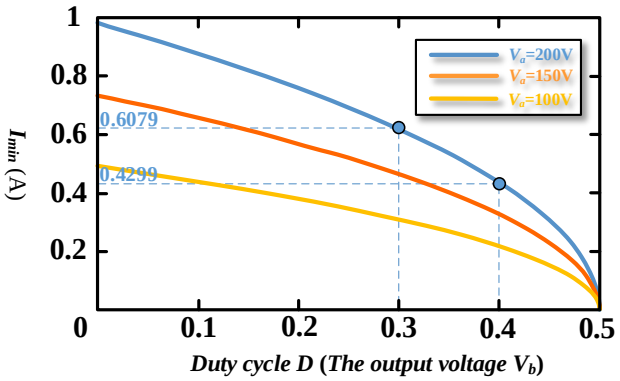


Fig. 6. The relationship curve between $I_{min}$ and duty cycle $D$.

When BCM converters operating in fixed reverse current, at present, the value of $I_R$ is 1 A.

When $I_{lower} = -I_R = -1$ A, the power of circulating energy is:

$$P_{\text{cir}} = \frac{1}{2}\cdot(V_a - V_b)\cdot\sqrt{1 - \frac{2\cdot C_{oss} V_a (V_a - 2\cdot V_b)}{L_f}} \tag{17}$$

However, when BCM converters operating in minimum negative current, the lower limit value of inductor current $I_{lower}$ will depend on the working conditions, rather than a constant value, and its dead time will also change.

When $I_{lower} = -I_{min}$, the power of circulating energy is:

$$P_{\text{cir}} = \frac{1}{2}\cdot(V_a - V_b)\cdot\sqrt{I_{min}^2 - \frac{2\cdot C_{oss} V_a (V_a - 2\cdot V_b)}{L_f}} = 0 \tag{18}$$

When the negative current is minimized in the condition of realizing ZVS, the power of circulating energy is minimized to zero, namely, the phenomenon of circulating energy is eliminated.

Furthermore, BCM converters operating in minimum negative current, the ripple of inductor current is reduced to a certain extent.

When BCM converters operating in fixed reverse current, the expression of ripple of inductor current is as follow:

$$\Delta i_f = 2\cdot(I_o + I_R) = 2\cdot\left(\frac{P_o}{DV_a} + \sqrt{\frac{2\cdot C_{oss} V_a^2}{L_f}}\right) \tag{19}$$

When BCM converters operating in minimum negative current, the expression of ripple of inductor current is as follow:

$$\begin{aligned}\Delta i_m &= 2\cdot(I_o + I_{\min}) \\ &= 2\cdot\left(\frac{P_o}{DV_a} + V_a\cdot\sqrt{\frac{2\cdot C_{oss}\cdot(1-2\cdot D)}{L_f}}\right)\end{aligned} \tag{20}$$

where, the output power $P_o$ = 100 W, the input voltage $V_a$ = 200 V, the output capacitance $C_{oss}$ = 462 pF and the filter inductor $L_f$ = 40 μF.

According to formula (19) and (20), the relationship between inductance current ripple and duty cycle is plotted as shown in Fig. 7. In conclusion, compared with BCM converters operating in fixed reverse current, BCM converters operating in minimum negative current mode eliminates the circulating energy and reduces the ripple of inductor current of BCM converters.

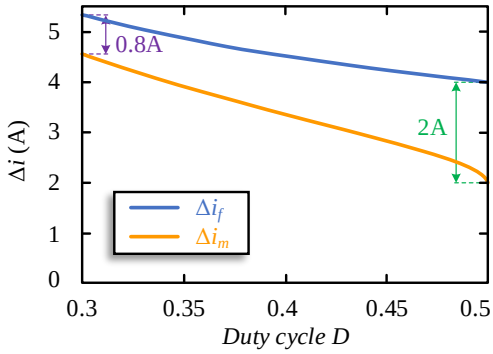


Fig. 7. The relationship between inductance current ripple $\Delta i$ and duty cycle $D$.

To balance the cost of control circuit and control precision, a control scheme which combinates software prediction and hardware comparison is adopted in this paper. That is, the on-time $t_{on}$ of $S_1$ in one switching period is obtained by predictive calculation, and its calculation expression is as follows:

$$t_{on} = L_f \cdot \frac{I_{upper} - I_{lower}}{V_a - V_b} \tag{21}$$

The time of $S_2$ is turned off is obtained by hardware comparison, and $S_2$ is turned off at the moment of current $i_L$ is less than $I_{lower}$. Then, $S_1$ is turned on after a period of dead zone. Therefore, the scheme not only has the advantages of flexible control, but also eliminates error accumulation and facilitates multi-channel interleaving control.

The optimal control diagram of BCM with minimum negative current is as shown in Fig. 8.

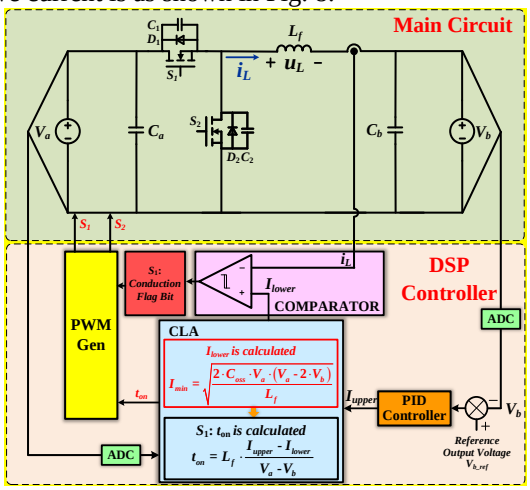


Fig. 8. The control diagram of BCM with minimum negative current.

The inductor current $i_L$, the input voltage $V_a$, and the output voltage $V_b$ are sampled, the output voltage outer loop is used as the reference for the output current inner loop by PID controller, and the conduction time $t_{on}$ of $S_1$ and the minimum negative current $I_{min}$ is calculated by the control law accelerator (CLA) of DSP. Then, the value of $I_{lower}$ (= $-I_{min}$) is fed into the analog comparator for comparing with $i_L$, and $S_2$ is turned off at the moment of current $i_L$ is less than $I_{lower}$. $S_1$ is turned on at the end of dead zone.

## IV. Experimental Results

The specifications and components of BCM synchronous buck converters are shown in Table I:

TABLE I
SPECIFICATIONS AND COMPONENTS OF BCM SYNCHRONOUS BUCK CONVERTERS

| Specifications and Components | | Value |
|---|---|---|
| | Power rating $P_o$ | 100 W |
| | Input voltage $V_a$ | 200 V |
| | Output voltage $V_b$ | 60 V, 100 V |
| | Filter inductor $L_f$ | 40 μH |
| Switches (STW75NF30) | On-state resistance $R_{ds(on)}$ | 45 mΩ |
| | Equivalent output capacitance $C_{oss}$ | 462 pF |
| | Total gate charge $Q_g$ | 164 nC |
| | filter capacitor $C_a$, $C_b$ | 47 μF |
| | Fixed reverse current $I_R$ | 1 A |

In order to verify the corresponding theoretical analysis, as shown in Fig.9, a 100W BCM synchronous buck converters experimental platform is built.

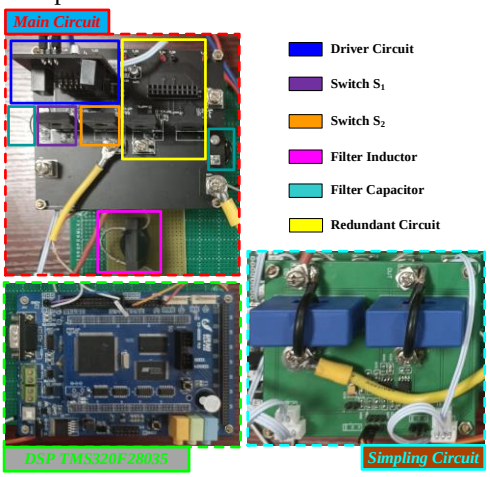


Fig. 9. Laboratory prototype of BCM synchronous buck converters.

### A. Experimental Waveforms

As shown in Fig.10, when the BCM synchronous buck converters operating in fixed reverse current, $I_{lower}$ is the fixed value, which is equal to $-I_R$.

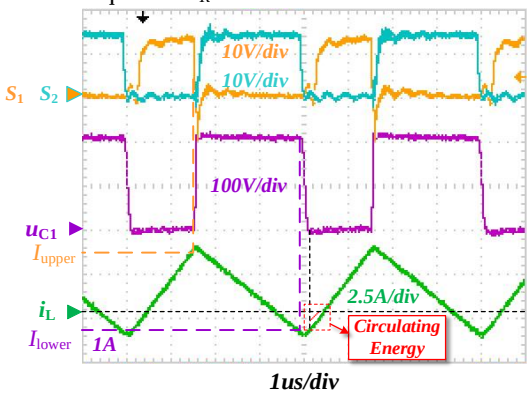


Fig. 10. Experimental waveforms of BCM synchronous buck converters with fixed reverse current.

In the time of dead zone, the drain-source voltage $u_{C1}$ of the $S_1$ drops to zero and is clamped to zero by the body diode, waiting for the drive signal of turning on the switch $S_1$ to realize ZVS. Therefore, synchronous buck converters operating in BCM, the feasibility of realizing ZVS is verified by the experimental results.

However, at the moment of $u_{C1}$ drops to zero, $i_L$ remains negative and the energy of main circuit flows from the output

side to the input side. Thus, BCM synchronous buck converters exists the phenomenon of circulating energy, which generates reactive power loss and reduces the efficiency of the converter.

In order to eliminate the problem of circulating energy, the optimal control strategy of minimum negative current is proposed in this paper. As shown in Fig. 11, when the BCM synchronous buck converters operating in minimum negative current, $I_{lower}$ is the variable, which changes with the output voltage.

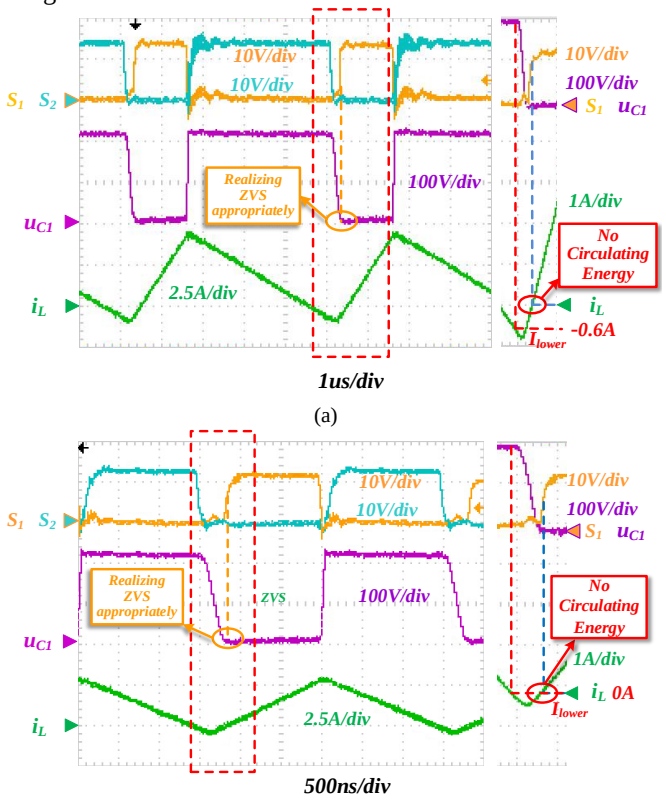


Fig. 11. Experimental waveforms of BCM synchronous buck converters with minimum negative current. (a) $V_b$ = 60 V. (b) $V_b$ = 100 V.

As shown in Fig. 11(a), when the output voltage $V_b$ = 60V, $I_{lower}$ is equal to -$I_{min}$ = -0.6 A. At the moment of $u_{C1}$ drops to zero, the inductor current $i_L$ is already zero, and the energy of main circuit does not flow from the output side to the input side after the body diode $D_1$ or the switch $S_1$ is turned on, and the phenomenon of circulating energy is eliminated. ZVS can be realized appropriately with the output voltage $V_b$ = 60V.

As shown in Fig. 11(b), when the output voltage $V_b$ = 100V, $I_{lower}$ is equal to -$I_{min}$ = 0 A. At the moment of $u_{C1}$ drops to zero, the inductor current $i_L$ has been zero. Therefore, the energy of main circuit doesn't flow from the output side to the input side after $D_1$ or $S_1$ is turned on, and the phenomenon of circulating energy is eliminated. That is, ZVS can be realized appropriately without negative current, which is similar to CRM converters. The feasibility and effectiveness of the proposed scheme of minimum negative current is verified by the experimental results.

Experimental waveforms of the load transition from half load to full load under the output voltage $V_b$=100V is presented in Fig. 12. It can be found that $V_b$ recovers to the normal level within a dozen switching cycles after the sudden change of load, and the controller keeps the output voltage stable and has good dynamic performance.

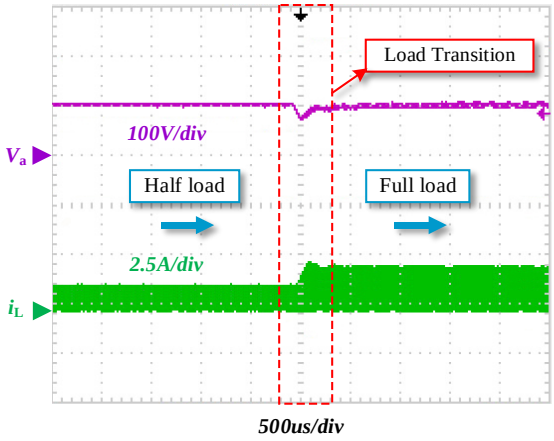


Fig. 12. Experimental waveforms of the load transition from half load to full load under the output voltage $V_b$=100V.

Fig. 13 shows the dynamic response of the inductor current when the output voltage is shift between 60 V and 100 V, and the controller has good dynamic performance and control effect.

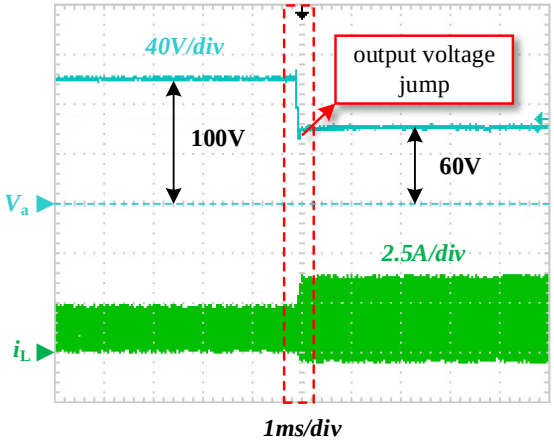


Fig. 13. The dynamic response of the inductor current when the output voltage is shift between 60 V and 100 V.

## B. Optimization Analysis

The efficiency of BCM synchronous buck converters under the control of different current modes is shown in Fig. 14.

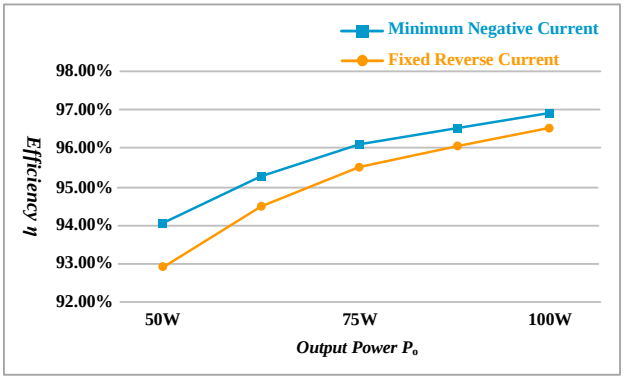


Fig. 14. Efficiency of BCM synchronous buck converters with different current mode ($V_a$ = 200V, $V_b$= 100V).

Compared with the fixed reverse current mode, minimum negative current mode improves the efficiency of BCM

converters. Especially, the optimization effect of the converter is more obvious in the condition of light load.

Fig. 15 shows the theoretically calculated loss breakdown of BCM synchronous buck converters with the output voltage $V_b$ = 100 V. Since BCM converters operating in minimum negative current reduces circulating energy, the conduction loss and turn-off loss of power switches and the copper losses and iron losses of inductor are reduced and the efficiency is improved.

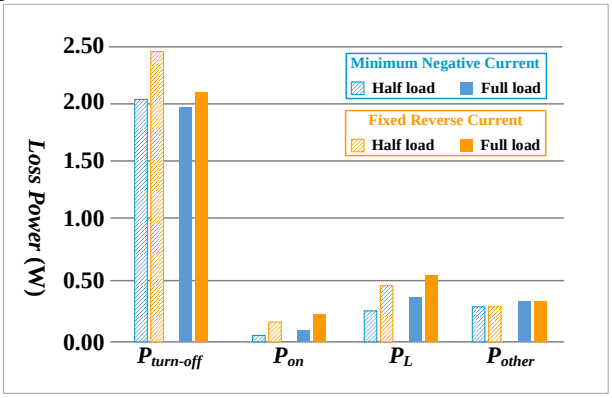


Fig. 15. The theoretically calculated loss breakdown of the two current modes with the output voltage $V_b$ = 100 V.

Fig. 16 presents the comparison of efficiency of BCM synchronous buck converters with the different output voltage under full load.

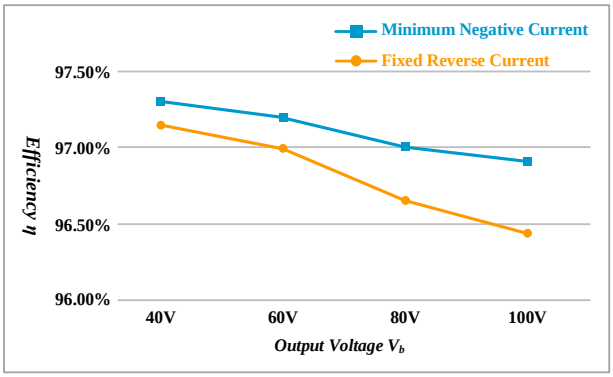


Fig. 16. The comparison of efficiency of BCM synchronous buck converters under the different output voltage.

## V. Conclusion

This paper mainly studies the optimization method of BCM converters. Taking synchronous buck converters as an example, the operating principle of BCM is briefly introduced. There is the phenomenon of circulating energy in BCM converters, which will reduce the efficiency of the converter. This paper analyzes the relationship between negative current and circulating energy and the optimization scheme of the circulating energy and the ripple of inductor current is proposed, namely, the minimum negative current optimization control scheme. The combination of software prediction and hardware comparison is adopted, and the corresponding control diagram is given, which improves the control flexibility and eliminates the error accumulation. Experiments validate the feasibility of realizing soft-switching in DC-DC converter under BCM, and the correctness of the optimal control scheme of the minimum negative current, which reduces circulating energy and the ripple of inductor current and improves the efficiency of the converter.

## References


[1] J. P. C. Silveira, P. J. d. S. Neto, M. V. de Paula, R. R. de Souza, T. A. d. S. Barros and E. R. Filho, "Evaluation of Bidirectional DC-DC Converter Topologies for Voltage Regulation in Hybrid Microgrids with Photovoltaic and Battery Technologies," *2018 13th IEEE International Conference on Industry Applications* (INDUSCON), 2018, pp. 215-221, doi: 10.1109/INDUSCON.2018.8627266.

[2] H. -S. Lee and J. -J. Yun, "High-Efficiency Bidirectional Buck–Boost Converter for Photovoltaic and Energy Storage Systems in a Smart Grid," in IEEE Transactions on Power Electronics, vol. 34, no. 5, pp. 4316-4328, May 2019, doi: 10.1109/TPEL.2018.2860059.

[3] Y. Zhang, X. Cheng, C. Yin and S. Cheng, "A Soft-Switching Bidirectional DC–DC Converter for the Battery Super-Capacitor Hybrid Energy Storage System," in IEEE Transactions on Industrial Electronics, vol. 65, no. 10, pp. 7856-7865, Oct. 2018, doi: 10.1109/TIE.2018.2798608.

[4] S. Sharifi, M. Jabbari and H. Farzanehfard, "A New Family of Single-Switch ZVS Resonant Converters," in *IEEE Transactions on Industrial Electronics*, vol. 64, no. 6, pp. 4539-4548, June 2017, doi: 10.1109/TIE.2017.2674632.

[5] M. R. Mohammadi and H. Farzanehfard, "A New Family of Zero-Voltage-Transition Nonisolated Bidirectional Converters With Simple Auxiliary Circuit," in *IEEE Transactions on Industrial Electronics*, vol. 63, no. 3, pp. 1519-1527, March 2016, doi: 10.1109/TIE.2015.2498907.

[6] M. R. Mohammadi, H. Farzanehfard and E. Adib, "Soft-Switching Bidirectional Buck/Boost Converter With a Lossless Passive Snubber," in *IEEE Transactions on Industrial Electronics*, vol. 67, no. 10, pp. 8363-8370, Oct. 2020, doi: 10.1109/TIE.2019.2947850..

[7] C. Marxgut, F. Krismer, D. Bortis and J. W. Kolar, "Ultraflat Interleaved Triangular Current Mode (TCM) Single-Phase PFC Rectifier," in *IEEE Transactions on Power Electronics*, vol. 29, no. 2, pp. 873-882, Feb. 2014, doi: 10.1109/TPEL.2013.2258941.

[8] X. Huang, F. C. Lee, Q. Li and W. Du, "High-Frequency High-Efficiency GaN-Based Interleaved CRM Bidirectional Buck/Boost Converter with Inverse Coupled Inductor," in *IEEE Transactions on Power Electronics*, vol. 31, no. 6, pp. 4343-4352, June 2016, doi: 10.1109/TPEL.2015.2476482.

[9] Q. Zhang, H. Hu, D. Zhang, X. Fang, Z. J. Shen and I. Bartarseh, "A Controlled-Type ZVS Technique Without Auxiliary Components for the Low Power DC/AC Inverter," in *IEEE Transactions on Power Electronics*, vol. 28, no. 7, pp. 3287-3296, July 2013, doi: 10.1109/TPEL.2012.2225075.

[10] C. -J. Chen, P. -Y. Wang, S. -T. Li, Y. -M. Chen and Y. -C. Chang, "An Integrated Driver with Bang-Bang Dead-Time Control and Charge Sharing Bootstrap Circuit for GaN Synchronous Buck Converter," in *IEEE Transactions on Power Electronics*, doi: 10.1109/TPEL.2022.3159717.

[11] X. Ren, Y. Zhou, Z. Guo, Y. Wu, Z. Zhang and Q. Chen, "Simple Analog-Based Accurate Variable On-Time Control for Critical Conduction Mode Boost Power Factor Correction Converters," in *IEEE Journal of Emerging and Selected Topics in Power Electronics*, vol. 8, no. 4, pp. 4025-4036, Dec. 2020, doi: 10.1109/JESTPE.2019.2926794.

[12] S. A. Gorji, A. Mostaan and M. Ektesabi, "A Comparative Study on PFC Bridgeless Flyback and SEPIC AC-DC Rectifiers Operating in DCM and BCM," *2019 IEEE 4th International Future Energy Electronics Conference* (IFEEC), 2019, pp. 1-6, doi: 10.1109/IFEEC47410.2019.9015037.

[13] Z. Zhang, J. Zhang, S. Shao and J. Zhang, "A High-Efficiency Single-Phase T-Type BCM Microinverter," in *IEEE Transactions on Power Electronics*, vol. 34, no. 1, pp. 984-995, Jan. 2019, doi: 10.1109/TPEL.2018.2824342.

[14] R. Pashaei, E. Babaei, C. Cecati and C. Buccella, "Analysis of Z-source based DC/DC converter in CCM, DCM and BCM operations," *2017 14th International Conference on Electrical Engineering/Electronics, Computer, Telecommunications and Information Technology* (ECTI-CON), 2017, pp. 777-780, doi: 10.1109/ECTICon.2017.8096354.